

Phase Transition Studies on BaTiO₃ and PbTiO₃ and Synthesis of Silicate Perovskite

BaTiO₃와 PbTiO₃에 대한 상전이 연구와 규산염 페로프스카이트의 합성

Young-Ho Kim(金榮浩)

Hawaii Institute of Geophysics, University of Hawaii at Manoa, Honolulu, Hawaii 96822

(하와이대학교 지구물리학 연구소)

ABSTRACT : Diamond anvil cell (DAC) interfaced with a YAG laser heating system has been used to study the phase transformations on perovskite structured titanates (BaTiO₃ and PbTiO₃) and to synthesize the silicate perovskite phase from the orthopyroxenes of MgSiO₃ and (Mg_{0.87}, Fe_{0.13})SiO₃. BaTiO₃ and PbTiO₃ transform from tetragonal phase to cubic at the pressures of approximately 2.6 GPa and 4.0 GPa at room temperature, respectively. Cubic phases of the both show wide range of stability in the extended in-situ high pressures and high temperature regions. Starting orthoenstatite of MgSiO₃ has yielded the perovskite phase as the major structure with ilmenite, gamma-spinel, beta-spinel and stishovite phases at ~38 GPa and ~1,000°C. (Mg_{0.87}, Fe_{0.13})SiO₃ has shown the perovskite as the major phase with beta-spinel, stishovite and enstatite phases at ~35 GPa and ~1,000°C. The ilmenite phase does not occur at this condition.

요약 : YAG (Yttrium Aluminum Garnet) 레이저와 다이아몬드엔빌셀(DAC)을 이용하여 페로프스카이트 구조물질중 BaTiO₃와 PbTiO₃에 대한 상전이의 MgSiO₃와 (Mg_{0.87}, Fe_{0.13})SiO₃ 성분인 사방휘석으로부터 규산염 페로프스카이트를 합성하였다. BaTiO₃와 PbTiO₃는 실온의 2.6 GPa와 4.0 GPa에서 각각 정방정계에서 등축정계로 상전이하며 고온, 고압하에서 매우 넓은 안정영역을 갖고 있다. MgSiO₃ 엔스테타이트를 출발물질로 하였을 경우 약 33 GPa, 1,000°C의 조건하에서 페로프스카이트가 주성분인데, 일메나이트, 감마스피넬, 스티쇼바이트도 부성분으로 나타난다. (Mg_{0.87}, Fe_{0.13}) SiO₃의 경우는 약 35 GPa와 1,000°C에서 페로프스카이트상이 주성분으로 나타나며, 베타스피넬, 스티쇼마이트와 본래 엔스테타이트상도 유지되나, 일메나이트상과 감마스피넬은 나타나지 않는다.

INTRODUCTION

There have been considerably abundant information and knowledge accumulated concerning the Earth's interior through the studies of geophysics. Principal issues in interpretation of these findings to the Earth interior are the following: 1) What are the mineral assemblages and their chemical compositions of the mantle and the core? 2) What is the temperature distribution through the earth's interior? 3)

What is the dynamic state(s) of those parts?

These questions are closely related with and dependent on each other. The equation of state (EOS) (i.e., pressure-volume-temperature relationship) and the possible phase transformations for the mantle phases are an important prerequisite for deducing a realistic earth model in terms of the mineralogy, chemical composition and thermal state (Jeanloz and Richter, 1979; Knittle et al., 1986).

Silicate perovskite is considered as the most abundant mineral phase in the lower mantle

irrespective of whether 670km seismic discontinuity is a chemical boundary, a phase boundary or the both (Knittle et al., 1986; Anderson and Bass, 1986; Liu and Bassett, 1986; Knittle and Jeanloz, 1987). Despite its consequences, there has been a limited number of studies in its physical properties since the first discovery of this phase (Liu, 1976). These might be due to the restricted pressure and temperature for the synthesis of this phase and the difficulties in generation of those conditions. Equation of state studies and thermal expansivity measurements on synthetic silicate perovskite have been done by Knittle and Jeanloz (1987), Hazen and Ross (1988) and Mao et al. (1988). However, all these works were performed in the restricted P-T conditions, and not well defined.

In view of abundance and consequence of the perovskite phases, synthesis of silicate perovskite has been performed from enstatite stoichiometries of MgSiO_3 and $(\text{Mg}_{0.87}, \text{Fe}_{0.13})\text{SiO}_3$ using DAC and YAG laser heating system. Furthermore, these techniques have been applied on some perovskite structure materials of titanates to survey whether they would show more stable phases under the extended high pressure and high temperature conditions. BaTiO_3 and PbTiO_3 have been studied in a DAC interfaced with YAG laser heating system. At room temperature, these were subjected to various pressures to re-investigate the first order phase transition using XRD, which have been extensively reported by many studies (Samara, 1966; Ikeda, 1975; Decker and Zhao, 1984; Jayaraman et al., 1984).

EXPERIMENTAL METHODS

Diamond is the hardest natural substance known to man, and especially transparent to electromagnetic (EM) radiation. These proper-

A BASSETT-TYPE DIAMOND ANVIL PRESSURE CELL

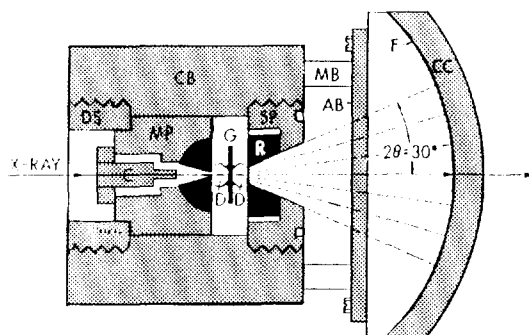


Fig. 1. A typical Bassett-type diamond anvil pressure cell. AB: Anvil Barrel, C: Collimator, CB: Cell Body, CC: Camera Cassette, D: Diamonds, DS: Driving Screw, F: Film, G: Gasket, MB: Mounting Bolt, MP: Moving Piston, R: Rocker, SP: Stationary Piston. Sample chamber is at center of gasket between two diamonds.

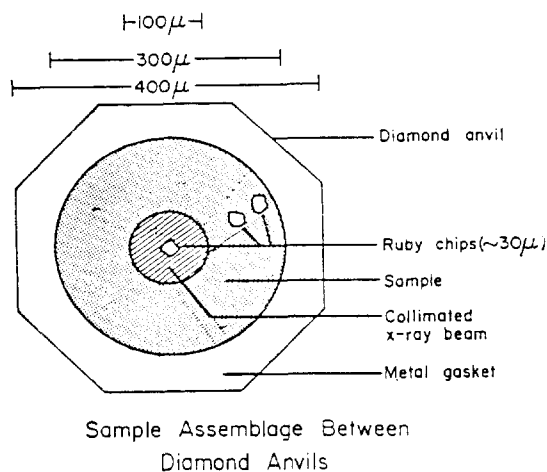


Fig. 2. A schematic sample assemblage between diamond anvils. Pressure gradient in sample chamber can be measured by distribution of several pieces of ruby.

ties are suitable for generation of high pressure and for X-ray radiation study. Bassett-type diamond anvil cells (Bassett et al., 1967; Ming and Manghnani, 1978) have been used for XRD through this study (Fig. 1).

The sample pressure is monitored using the ruby fluorescence method (Barnett et al., 1973).

A tiny chip of ruby of 10 to 30 μ m size in diameter is placed at the center of the sample chamber confined by metal gasket of Inconel 718 alloy (Fig. 2). Hydrostaticity of sample pressure for BaTiO₃ was maintained using the liquid mixture of 4:1 of methanol and ethanol. A typical pressure calibration system of ruby fluorescence is given (Fig. 3). When the synthesis was performed, the pressure of sample was estimated by the pre-established calibration of DAC with respect to the pressure. The purpose of this is to prevent the phase from contaminating by ruby. This kind of calibration is described elsewhere (Kim et al., 1988).

There are two systems for high temperature generation with the DACs: 1) electrical resistivity heating system. 2) YAG laser heating system. The latter has been used through this work. Bassett-type DACs are suitable for YAG laser heating system (Fig. 4). Since the introduction of YAG laser matched to DAC (Ming

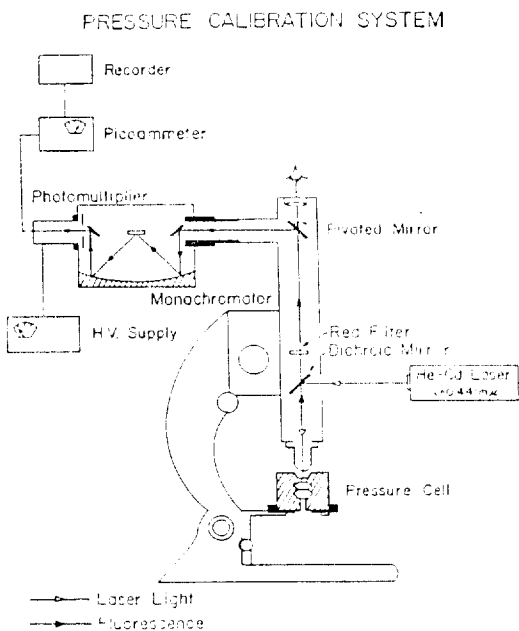


Fig. 3. A plane view of pressure calibration system. Ruby chip is used at the center of sample chamber in DAC as pressure calibrant.

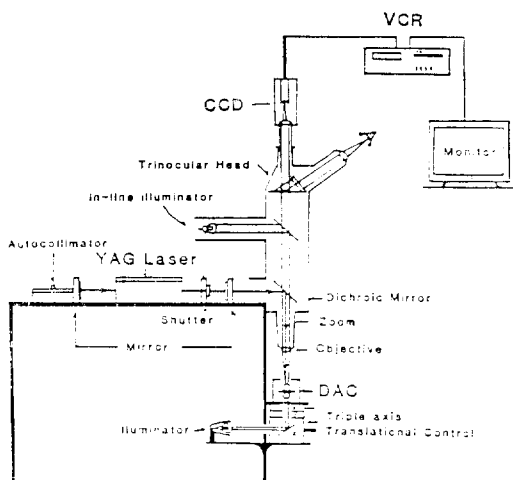


Fig. 4. A plane view of YAG laser heating system. Recently, VCR (Video Cassette Recorder), CCD (Charge Coupled Device) camera and TV monitor were installed. Therefore, the change of sample color by laser heating spot can be recorded in video tape as well as observed by naked eye through the microscope.

and Bassett, 1974), it has been improved to attain the temperatures of up to 7,000 $^{\circ}$ K with a high power YAG laser system (Heinz and Jeanloz, 1987). Sample temperature can be estimated on the basis of the intensities of incandescence emitted from the sample using an optical pyrometer (Ming and Bassett, 1974). PbTiO₃ absorbs laser at wavelength of 1.06 μ m without any heat absorbent added. Heating temperature of PbTiO₃ was estimated to be approximately 1,200 $^{\circ}$ C. On the other hand, BaTiO₃ is transparent to laser without absorbent. Powder of either platinum black (Pt) or graphite (C) is used as the heat absorbent of laser in addition to the transparent sample of 1 to 2% volume fraction. For synthesis of the silicate perovskite phase, the starting orthoestatite was mixed thoroughly with graphite. Sample temperature for these two was estimated to be approximately 1,000 $^{\circ}$ C.

RESULTS AND DISCUSSIONS

Perovskite Structures

BaTiO₃: Powder sample with the purity of 99.6% was obtained and identified as a tetragonal crystal system with lattice parameters of $a=4.057(54)\text{\AA}$ and $c=4.002(33)\text{\AA}$ at ambient conditions.

Since the first discovery of ferroelectricity in BaTiO₃, extensive investigations on titanates were conducted by applicability of this property to industry. Most of the study were concentrated on the high dielectricity and ferroelectric behaviour under temperatures at atmospheric pressure (Galasso, 1969). The phase transition from tetragonal to cubic perovskite corresponds

to that from ferroelectric to paraelectric. Transition pressure changes from 1 GPa to 2.8 GPa according to different experimental methods (i.e., 1.0 GPa by Curie point measurement, 1.9 GPa by Raman spectroscopy, 2.8 GPa by dielectric constant measurement) (Jayaraman et al., 1984).

At room temperature, two independent runs were made; one for quick check whether it transforms or not in the higher pressure region, and the other for re-investigation of transition pressures at room temperature and when it is heated by YAG laser. For quick check, pressure was loaded to 7.1 GPa, 19.7 GPa, and 33.0 GPa. We could assign a cubic lattice at 7.1 GPa by the shift of d-spacing of (200) XRD line, with $a=3.985(8)\text{\AA}$ and $V_m=38.11(6)$

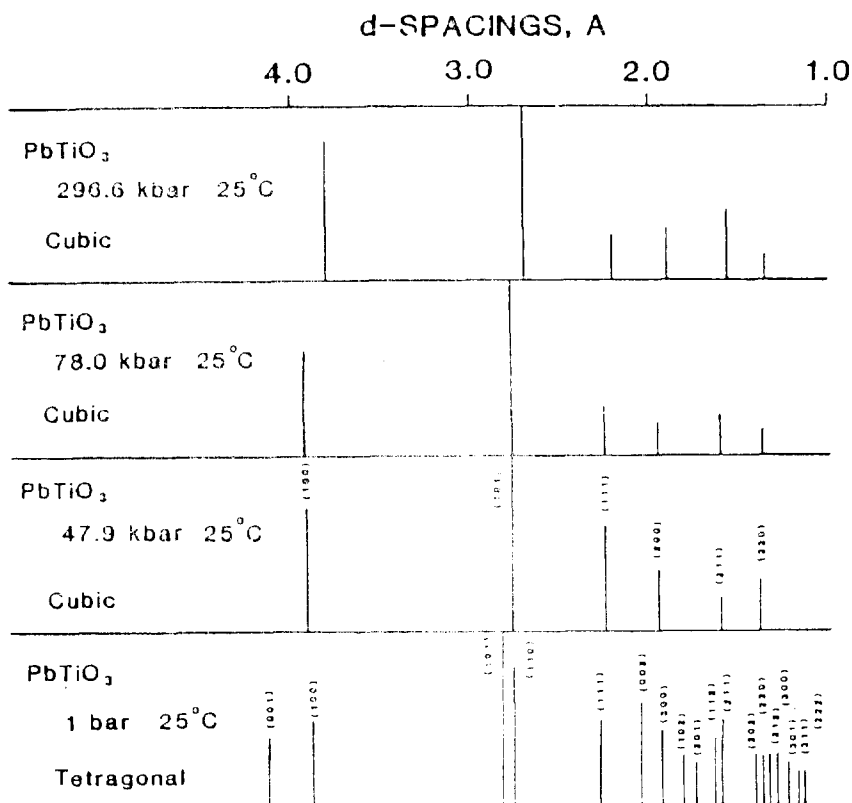


Fig. 5. XRD data for BaTiO₃ at 1 bar and high pressures at room temperature. Note phase transition from tetragonal system to cubic.

cm³/mole when Z=1. This cubic phase maintains to ~33.0 GPa (Fig. 5). For recheck the pressure of 1st order phase transition under truly hydrostatic pressure, sample was contained in gasket hole with a mixture of alcohols, then pressurized to prevent it from evaporation.

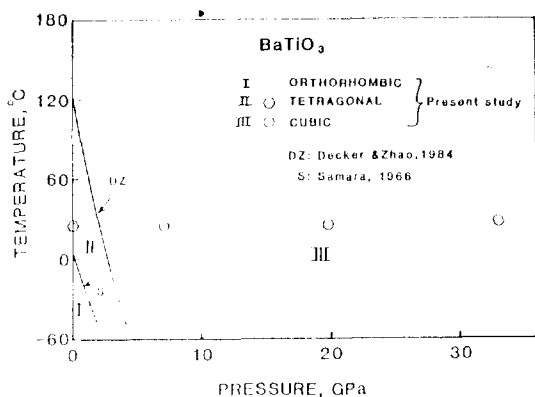


Fig. 6. Phase diagram for BaTiO₃. Pressure region was expanded up to 33 GPa at this study. Cubic phase shows wide stability under high pressures at room temperature.

XRD pattern from this first run shows that phase transformation already takes place, and this pressure was estimated to be 2.6 GPa. Therefore, it shows the phase transformation pressure occurs lower than 2.6 GPa. This cubic phase was subjected to be searched on its behaviour under high temperatures, mixed with either a small amount of graphite or platinum black by YAG system. This was transparent to the laser. Phase diagram was extended to higher pressure regions based on this study with previously reported data (Fig. 6).

PbTiO₃: This crystallizes in tetragonal structure at ambient conditions. Lattice parameters are: a=3.398(7)Å, c=4.141 (13)Å, V_m=18.943cm³/mole when Z=1. This tetragonal phase transforms into cubic structure at about 5.8 GPa (Ikeda, 1975). This transition pressure was derived from the measurement of capacitance versus pressure. Sample pressure was monitored by the known phase transition

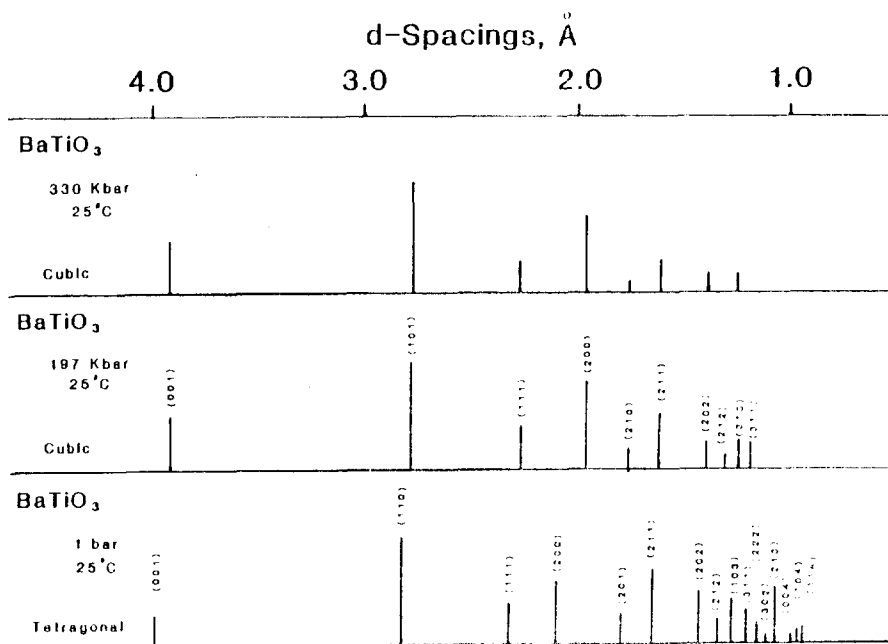


Fig. 7. XRD data for PbTiO₃ at 1 bar and high pressures at room temperature. Note phase transition starting tetragonal system to cubic.

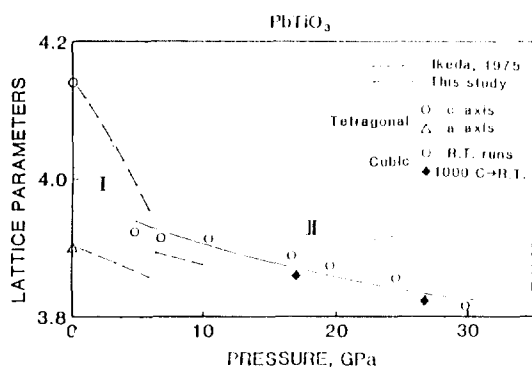


Fig. 8. Lattice parameters vs. high pressures. The results of this study is compared with Ikeda's. His estimation of phase transition pressure of tetragonal phase to cubic phase is higher than that of this study. Two runs using laser heating are also shown in cubic crystal system.

pressures (i.e., Bi I ~ II, Ti II ~ III and Ba phase transitions) in cubic anvil-type apparatus. In this experiment, ruby fluorescence method was used for pressure calibration. Cubic phase was identified at the pressure of 4.8 GPa (Fig. 7). The lattice parameter at this pressure is 3.923(13) Å. The pressure was increased at approximately 5 GPa interval up to 29.7 GPa. Cubic phase is maintained up to this high pressure (Fig. 8). The zero pressure volume of this cubic phase was calculated to be 36.54 cm³/mole by fitting the compression data polynomially since this high pressure phase is not quenchable. Bulk modulus is calculated to be 382(42) GPa assuming $K'=4$.

This specimen was heated using YAG laser system at two pressures of 17.0 GPa and 26.7 GPa. Sample pressures on both runs were taken the average values of before and after heating. There are no phase change detected, but volume at each pressure appears lower than those of the unheated cases. It is known that PbTiO₃ shows the negative thermal expansivity at near room temperature to 700°K, and changes to the

positive at 800°K (Chu et al., 1987). At 763°K, the crystal structure changes from tetragonal ferroelectric to cubic paraelectric. Reduction of volume after laser heating might be induced by this negative thermal expansion in the light of the drawbacks of laser usage (i.e., 1) inaccuracy in estimation of sample temperature by incandescence, 2) inhomogeneity of temperature distribution in laser beam, 3) irregulation of focal distances and so on). It would be of value to verify this property at in situ high pressure and high temperature conditions simultaneously using white X-ray source with a specially disigned DAC (Manghnani et al., 1985).

A Raman spectral study indicates the ferroelectric to paraelectric transition near 11 GPa at room temperature. This pressure was derived by extrapolation from a high temperature phase transition studies conducted at 12.5 GPa to room temperature conditions (Jayaraman et al., 1984). There appear no intimate relations in phase transition pressure between the result of Raman spectroscopy and that of capacitance measurements. Based on the present XRD results, it would be proposed that phase transforms from tetragonal to cubic at a pressure of lower than 4.8 GPa.

Synthesis of Silicate Perovskites

The starting pyroxene phases of orthopyroxenes (MgSiO₃ and (Mg_{0.87}, Fe_{0.13}) SiO₃) were synthesized at Geophysical Laboratory in Carnegie Institution. Unloaded product from DAC after heating was transferred to the modified Debye Scherrer camera (114.6mm diameter), then X-rayed for about 100 hours using Cu K α radiation. All pressures shown here are those before laser heating.

MgSiO₃ stoichiometry: Lattice parameters at ambient conditions are determined using

114.6mm diameter Debye Scherrer camera: $a=18.204\text{\AA}$, $b=8.845\text{\AA}$, $c=5.197\text{\AA}$.

Approximately 25 GPa run has shown that enstatite is the major phase with a broad band at a d-spacing of 2.5\AA . The other run at ~ 30 GPa has yielded a mixture of beta spinel, stishovite, and ilmenite phase. At this run, instead of wide band at that position, three sharp lines have appear, and are assigned as ilmenite (104), β -spinel (141) and the sustained starting phase. Identifications of these phases were based on the comparisons of the relative

intensities and the d-spacings with those of the published (Ringwood and Major, 1970; Moore and Smith, 1970; Liu, 1976; ASTM Card Catalogue 15~26). Since there appear many diffraction lines and some of them are superimposed other, it is hard to estimate the transition pressure and which phases are really existed in the mixture of diffraction lines. However, the detailed descriptions of these transient phases were skipped in this study because main target of this work is the production of perovskite phase.

Table 1. MgSiO_3 at 0.0001 GPa quenched from approximately 38 GPa (before heating) and heated by YAG laser system at the temperature of $\sim 1,000^\circ\text{C}$.

I/I_0^*	d, obs.	Phases	Lattice parameters
5	4.125	?	
35	3.438	p (110)	
15	3.201	b (211)	gamma-spinel
10	3.083	p (111)	$a=8.159(58)$
10	2.970	st(110)	
5	2.786	?	stishovite
10**	2.555	i (104)	$a=4.190(11)$
100	2.443	p (112)/ b (141) ? / g (311) ?	$c=2.646(21)$
10	2.409	p (200)	
35**	2.068	p (103)/ p (211)/ i (113)	beta-spinel***
30	2.015	p (022)/ b (042)	$a=8.028$
35	1.968	p (202)/ st(111)	$b=11.464$
20	1.920	p (113) ?	$c=5.670$
15	1.858	p (122)/ st(210)/ g (331)	
90	1.725	p (220)/ p (004)	ilmenite***
15**	1.669	p (221)/ g (422)	$a=4.733$
15	1.618	i (116), (205)	$c=13.248$
10	1.541	p (114)/ st(211)	
20	1.515	p (131)	perovskite
20**	1.483	p (311)/ st(220)	$a=4.796(9)$
50	1.421	p (132)/ b (442)	$b=4.947(13)$
60	1.392	p (312)/ i (030)/ g (531)	$c=6.915(12)$
10	1.294	p (133)/ i (119)/ g (620)	
30	1.221	p (224)	

*Determined visually

**XRD lines appear wide in photographic film

***Not constrained well

Two runs, at approximately 35 GPa and 37 GPa have shown the appearance of the perovskite phase. At 35 GPa, gamma-spinel, stishovite, ilmenite, and perovskite are the abundant phases in an equal amount with several weak enstatite lines and a few unidentified lines. Generally, lines at lower angle region were clearly identified. On the other hand, almost all lines at higher angle region were assigned as the mixture of several phases. At 37 GPa, the relative intensities and the number of diffraction lines for perovskite increase very much compared with stishovite, β -spinel, γ -spinel, and ilmenite. Enstatite disappears completely at this

pressure. At the estimated pressure of 38 GPa, perovskite becomes the definite major phase, and γ -spinel as a secondary with a reduced number of β -spinel. Stishovite remains in all runs, and ilmenite phase is not well constrained at this pressure (Table 1).

($Mg_{0.87}Fe_{0.13}$) SiO_3 : The enstatite solid solution contains 13% of iron, and the lattice parameters are $a=18.316\text{\AA}$, $b=8.840\text{\AA}$, $c=5.191\text{\AA}$ at ambient conditions.

At approximately 35 GPa, perovskite appears as the major phase with some β -spinel and stishovite. Lattice parameters of each phases present in this run were listed in Table 2.

Table 2. ($Mg_{0.87}, Fe_{0.13}$) SiO_3 at 0.0001 GPa quenched from approximately 35 GPa (before heating) and heated by YAG laser system at temperature of $\sim 1,000^\circ\text{C}$.

I/I_0^*	d, obs.	Phases	Lattice parameters
12	3.447	p (110)	
10	3.326	b (220)/ e (121)	enstatite***
30	3.190	e (420), (221)/ b (211)	a =18.265
40	2.985	st(110)	b =8.706
25	2.881	b (040)/ G (220)/ e (610)	c =5.462
10	2.554	e (131)	
100	2.443	p (112)	beta-spinel
10	2.404	p (200)	a =8.244(55)
30	2.093	e (630)/ p (103)	b =11.541(68)
20	2.013	p (022)/st(111)	c =5.638(65)
10	1.918	p (113)	
15**	1.854	p (122)	stishovite
80	1.725	p (220)	a =4.208(20)
15**	1.610	e (10, 21)	c =2.700(70)
10	1.519	p (131)/st(211)	
15	1.484	b (451)/st(220)	perovskite
25	1.422	p (132)	a =4.736(37)
10	1.398	p (204)	b =4.950(31)
5	1.374	b (253)/ p (312)	c =6.953(44)
10	1.295	p (133)	
10	1.236	p (040)/st(301)	
20	1.221	p (224)	

*Determined visually

**XRD lines appear wide in film

***Not constrained well

There is no ilmenite phase in this composition, contrasting to very wide stability region in the Mg end-member enstatite. This result follows the high pressure phase relationships in the $\text{MgSiO}_3\text{-FeSiO}_3$ system at $\sim 1,000^\circ\text{C}$, which have been established confidently by the successive experimental facts (Liu and Bassett, 1986).

Production of perovskite is essential to physical and chemical measurement of this phase, and is largely dependent on the generation of high pressures and temperatures, and maintaining the condition through the process of synthesis. The accurate equation of the state, phase transformation if any, and thermal expansivity of this phase are of the critical parameters to deduce a realistic model of the earth interior. This is a next requirement to the synthesis of silicate perovskite.

SUMMARY

1. BaTiO_3 (perovskite structure) transforms from tetragonal to cubic structure below 2.6 GPa, and this cubic phase shows a wide stability range up to 33 GPa at room temperature. The specimen is transparent to the laser. Perovskite type PbTiO_3 transforms from tetragonal to cubic structure at approximately 4 GPa. This cubic phase maintains up to 30 GPa. Transition pressure observed in this study appears much lower than that by Raman spectroscopy study and capacitance measurements. Negative thermal expansivity of this phase is not well constrained for the quenchability of laser heating system.

2. In the synthesis of silicate perovskite, the final product from MgSiO_3 is the mixed phase of perovskite with ilmenite, γ -spinel, β -spinel and stishovite. On the other hand, $(\text{Mg}_{0.87}, \text{Fe}_{0.13})\text{SiO}_3$ yielded the mixture of perovskite, β -spinel, and stishovite without ilmenite phase.

It is crucial to determine the physical property of this phase for geophysical modelling of the earth in the light of its abundance in the interior of the planet, but available measured values lack.

Acknowledgement: Thanks are due to John Balogh for his experimental supports and maintenance of equipments. The author appreciates L.C. Ming and M.H. Manghnani for their comments on experimental data. All experiments for this study were done in High-Pressure Laboratory, Hawaii Institute of Geophysics, University of Hawaii.

REFERENCES

- Anderson, D.L. and Bass, J.D. (1986) Transition region of the earth's upper mantle. *Nature*, 320, 321-328.
- Barnett, J.D., Block, S., and Piermarini, G.J. (1973) An optical fluorescence system for quantitative pressure measurement in diamond anvil cell. *Rev. Sci. Instrum.*, 44, 1-9.
- Basset, W.A., Takahashi, T., and Stook, P. (1967) X-ray diffraction and optical observations of crystalline solids up to 300 kbars. *Rev. Sci. Instrum.*, 38, 37-42.
- Chu, C.N., Saka, N., and Suh, N.P. (1987); Negative thermal expansion ceramics: *Rev. Mat. Sci. & Eng.*, 95, 303-308.
- Galasso F.S. (1969) *Structure, Properties and Preparation of Perovskite-Type Compounds*. Pergamon Press Inc.
- Hazen, R.M. and Ross, N.L. (1988) Thermal expansion study of MgSiO_3 perovskite. *Eos*, 69, 473.
- Heinz, D.L. and Jeanloz, R. (1987) Temperature measurements in the laser-heated diamond cell. *High-Pressure Research in Mineral Physics*, Edited by M.H. Manghnani and

- Y. Syono, 113-128.
- Ikeda, T. (1975) Effect of hydrostatic pressure on the phase transition of ferroelectric PbTiO_3 . *Solid State Commun.*, 16, 103-104.
- Jayaraman, A., Remeika, J.P., and Katiyar, R. S. (1984) A high pressure raman study of the ferroelectric to paraelectric transition in BaTiO_3 and PbTiO_3 . *Mat. Res. Soc. Symp. Proc.*, 22, 165-168.
- Jeanloz, R. and Richter, F.M. (1979) Convection, composition and thermal state of the lower mantle. *J.G.R.*, 84(B10), 5497-5503.
- Kim, Y.H., Ming, L.C., and Manghnani, M.H. (1988) High pressure and high temperature phase transformation studies on hedenbergite ($\text{Ca}(\text{Fe}, \text{Mn})\text{Si}_2\text{O}_6$), submitted to EOS, AGU.
- Knittle, E., Jeanloz, R., and Smith, G.L. (1986) Thermal expansion of silicate perovskite and stratification of the earth's mantle. *Nature*, 319, 214-216.
- Knittle, E. and Jeanloz, R. (1987) Synthesis and equation of state of $(\text{Mg}, \text{Fe}) \text{SiO}_3$ perovskite to over 100 gigapascals. *Science*, 235, 668-670.
- Liu, L.-G. (1976) The high-pressure phases of MgSiO_3 . *Earth Planet. Sci. Lett.*, 31, 200-208.
- Liu, L.-G. and Bassett, W.A. (1986) *Elements, Oxides, and Silicates: High Pressure Phases with Implications for the Earth's Interior*. Oxford University Press.
- Mao H.K., Shu, A., Jephcoat, A., Hemley, R.J., Chen, L., Wu, Y., and Bassett, W.A. (1988) Compressibility and thermal expansion of $(\text{Mg}, \text{Fe}) \text{SiO}_3$ perovskite at high hydrostatic pressures. *EOS*, 69, 494-495.
- Manghnani, M.H., Ming, L.C., Balogh, J., Qadri, S.B., Skelton, E.F., and Schiferl, D. (1985) Equation of state and phase transition studies under in-situ high P-T conditions using synchrotron radiation, *SOLID STATE PHYSICS UNDER PRESSURES: Recent Advance with Anvil Devices*, Edited by S. Minomura, 343-350.
- Ming, L.C. and Bassett, W.A. (1974) Laser heating in the diamond anvil press up to 2,000°C sustained and 3,000°C pulsed at pressures up to 260 kilobars. *Rev. Sci. Instrum.*, 45, 1115-1118.
- Ming L.C. and Manghnani, M.H. (1978) Isothermal compression of bcc transition metals to 100 kbar. *Jour. Appl. Phys.*, 49, 208-212.
- Moore, P.B. and Smith, J.V. (1970) Crystal structure of $\beta\text{-Mg}_2\text{SiO}_4$: crystal-chemical and geophysical implications. *Phys. Earth Planet. Int.*, 3, 166-177.
- Ringwood, A.E. and Major, A. (1971) Synthesis of majorite and other high pressure garnets and perovskites. *Earth Planet. Sci. Lett.* 12, 411-418.
- Samara, G.A. (1966) Pressure and temperature dependences of the dielectric properties of the perovskite BaTiO_3 and SrTiO_3 . *Phys. Rev.*, 151, 378-386.